Bioorganic & Medicinal Chemistry 20 (2012) 6870–6876

Contents lists available at SciVerse ScienceDirect

Bioorganic & Medicinal Chemistry

journal homepage: www.elsevier.com/locate/bmc

Control of leakage activities of alamethicin analogs by metals: Side chain-dependent adverse gating response to Zn^{2+}

Daisuke Noshiro, Koji Asami, Shiroh Futaki *

Institute for Chemical Research, Kyoto University, Uji, Kyoto 611-0011, Japan

ARTICLE INFO

Article history:
Received 23 August 2012
Revised 16 September 2012
Accepted 17 September 2012
Available online 28 September 2012

Keywords:
Alamethicin
α-Aminoisobutyric acid (Aib)
Histidine
Leakage assay
Zn^{2+}-coordination

ABSTRACT

Alamethicin (Alm), an antimicrobial peptide rich in α-aminoisobutyric acid (Aib), is known to self-assemble to form channels in the membranes. Previously, we reported that HG-Alm, an Alm analog with a single His residue at the N-terminus, forms channel assemblies with extremely long lifetimes in the presence of Zn^{2+}. In this study, HG-Alm analogs, in the sequences of which all Aib residues were substituted by Leu, norvaline (Nva), or norleucine (Nle), were synthesized and their leakage activities were measured using fluorescent dye-loaded liposomes. We found that these peptides could be categorized into two classes with different gating responses to Zn^{2+}.

1. Introduction

Alamethicin (Alm: acetyl-Aib-Pro-Aib-Ala-Aib-Ala-Gln-Aib-Val-Aib-Gly-Leu-Aib-Pro-Val-Aib-Aib-Glu-Gln-Phol (Phol = phenylalaninol)), a 20-residue helical peptide rich in α-aminoisobutyric acid (Aib), is a member of the channel-forming antimicrobial peptides known as peptaibols.[1] Alm self-associates in lipid bilayers to form channels, through which ions and small molecules penetrate. The channels are formed by assembly of a variable number of monomers surrounding a central pore, and the mechanisms of channel formation can be understood in terms of the barrel-stave model.[2–4] Several studies have focused on the potential use of Alm channels as sensing platforms.[5–9] Previously, we synthesized HG-Alm, an Alm analog with a single His residue via a Gly spacer at the N-terminus. (Fig. 1)[10]. Stabilization of larger channel assemblies (8-, 10-, and 12-mer assemblies) by Zn^{2+}-coordination with histidyl imidazoles and N-terminal amino groups and the potential applicability of HG-Alm for metal sensing were demonstrated.

Alm has also been used for membrane permeabilization, which enables transport of polar and charged molecules across the membrane; successful measurement of the activity of membrane-bound enzymes, including Ca^{2+}-dependent ATPase and UDP-glucuronosyltransferase, was achieved by membrane permeation of the substrates and reactants for these enzymes using Alm.[11,12] Permeation of membranes by Alm was also employed to supply substrates to the enzymes encapsulated in lipid-vesicular microreactors.[13] The development of Alm analogs, the membrane transport of which is controllable by external stimuli, such as metal ions, may therefore have impacts on the development of novel assay systems and controlled-release systems. Zn(II)-mediated inhibition of carboxyfluorescein (CF) leakage from CF-loaded unilamellar vesicles was reported for the peptaibol trichogin tethered on a tripodal template to form a complex with Zn(II).[14]

In the present study, we synthesized HG-Alm analogs, where all Aib residues of HG-Alm were substituted with Leu, norvaline (Nva), or norleucine (Nle), and their membrane-permeabilizing abilities were compared with that of HG-Alm (Fig. 1). Although HG-Alm may serve as a metal-responsive membrane-permeabilizing agent, preparation of Aib-containing peptides is difficult using ordinary procedures for Fmoc-solid-phase peptide synthesis due to the steric hindrance of Aib at the alpha carbon. Therefore, the availability of Alm analogues or variants without Aib residues would benefit functional design and studies of channel-forming and membrane-interacting molecules based on Alm. The membrane-permeabilizing abilities of these Aib analogs were evaluated using liposomes loaded with the fluorescent dye 8-aminonaphthalene-1,3,6-trisulfonic disodium salt (ANTS) and its quencher *p*-xylene-bis-(N-pyridinium) bromide (DPX), based on the increment of fluorescent intensity of ANTS liberated from liposomes in the presence of these Alm analogs. Unexpectedly, Zn^{2+} had the opposite effect on ANTS/DPX leakage by these peptides; Zn^{2+} accelerated the leakage induced by HG-Alm and HG-[Nva]Alm but blocked the leakage by HG-[Leu]Alm and HG-[Nle]Alm. Thus, we demonstrated that the membrane-permeabilizing abilities of these peptides were reversibly controllable by the addition and removal of Zn^{2+}.

* Corresponding author. Tel.: +81 774 38 3210; fax: +81 774 32 3038.
E-mail address: futaki@scl.kyoto-u.ac.jp (S. Futaki).

0968-0896/$ - see front matter © 2012 Elsevier Ltd. All rights reserved.
http://dx.doi.org/10.1016/j.bmc.2012.09.046

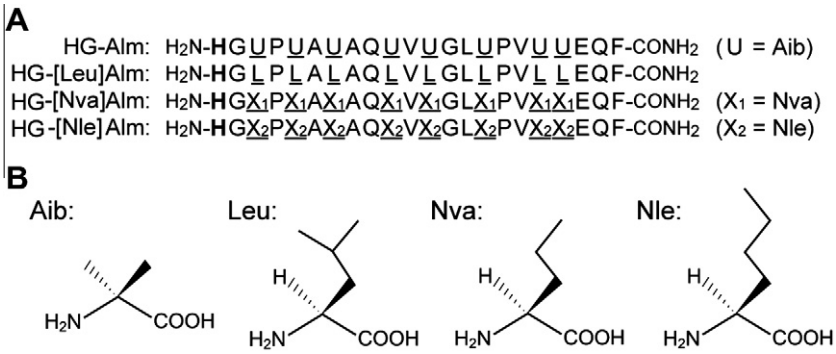

Figure 1. (A) The amino acid sequences of HG-Alm and its analogs used in this study. (B) The chemical structures of Aib, Leu, Nva, and Nle.

2. Results

2.1. ANTS/DPX leakage induced by HG-Alm

We employed 1-palmitoyl-2-oleoylphosphatidylcholine (POPC) large unilamellar vesicles (LUVs) containing ANTS together with a fluorescence quencher, DPX, to assess the membrane-permeabilizing activities of Alm analogs. Permeabilization of LUVs leads to the release of ANTS/DPX from LUVs. Release of ANTS and DPX from liposomes abolishes the quenching of DPX, and there is an eventual increase in fluorescence intensity of ANTS.[15] We assessed the membrane-permeabilizing abilities of the Alm analogs by the increase in fluorescence for 5 min after addition of each peptide.

We first determined the membrane-permeabilizing activities of HG-Alm (Fig. 2) in the absence or presence of Zn^{2+}. Figure 2A shows the percent leakage after addition of HG-Alm as a function of the peptide-to-lipid molar ratio (P/L) on a logarithmic scale. In the absence of Zn^{2+}, HG-Alm induced 50% leakage in the P/L range 0.02–0.03. On the other hand, in the presence of Zn^{2+}, HG-Alm induced 50% leakage in the P/L of ~0.01, indicating that Zn^{2+} enhanced the membrane-permeabilizing ability of HG-Alm. Figure 2B shows the successive switch of ANTS/DPX leakage using HG-Alm (P/L = 0.006) by the addition and removal of Zn^{2+} to/from the sample solution. As shown in the figure, addition of Zn^{2+} accelerated the leakage, while the removal of Zn^{2+} by EDTA stopped the leakage, demonstrating to the effective control of leakage by Zn^{2+}.

2.2. ANTS/DPX leakage induced by HG-[Leu]Alm

The sequence of Alm includes eight Aib residues. ANTS/DPX leakage can be promoted by pore formation due to the self-assembly of Alm in the liposomal membranes. Aib is considered to be important for the formation of the helical structure and pore formation.[16] Due to the steric hindrance at the alpha carbon with two methyl groups, construction of the Alm peptide chain by the standard coupling protocol in solid-phase peptide synthesis is problematic due to the formation of deletion peptides. On the other hand, Spach and co-workers previously synthesized an alamethicin analog in which all Aib residues were substituted with Leu residues, Alm-dUL (acetyl-Leu-Pro-Leu-Ala-Leu-Ala-Gln-Leu-Val-Leu-Gly-Leu-Leu-Pro-Val-Leu-Leu-Glu-Gln-Phol), and showed that Alm-dUL also forms voltage-dependent channels in planar lipid membranes with a lifetime ~1/10 that of Alm.[17] Considering the ease of synthesis, we next synthesized an HG-Alm analog in which all Aib residues were substituted with Leu residues, HG-[Leu]Alm (Fig. 1), and examined whether HG-[Leu]Alm could also be used for membrane permeabilization.

Figure 2C shows the results of a leakage assay using HG-[Leu]Alm. In the absence of Zn^{2+}, HG-[Leu]Alm induced 50% leakage in the P/L range 0.0002–0.0004, which was about two orders of magnitude lower than HG-Alm, indicating that HG-[Leu]Alm has greater membrane-permeabilizing ability than HG-Alm. However, there was a marked difference compared to HG-Alm, which induced leakage in the presence of Zn^{2+}, and the addition of 50 μM $ZnCl_2$ led to a considerable decrease in the membrane-permeabilizing activity of HG-[Leu]Alm, yielding less than 5% leakage even at a P/L of 0.1. Figure 2D shows leakage control using HG-[Leu]Alm (P/L = 0.0008) in the same way as Figure 2B. In contrast to the case of HG-Alm, addition of Zn^{2+} stopped the leakage, while removal of Zn^{2+} increased the leakage.

To confirm the importance of the His residue for leakage control, we analyzed G-Alm and G-[Leu]Alm, which lacked the His residues at their N-termini. The addition of Zn^{2+} had no effect on the membrane-permeabilizing activities of G-Alm and G-[Leu]Alm, confirming the contribution of the His residue to the response to Zn^{2+} (Supplementary data Fig. 1).

2.3. Leakage and channel-forming activities of dimerized Alm and [Leu]Alm peptides

In our previous study, HG-Alm was shown to form dimer-based channel assemblies stabilized by Zn^{2+}-coordination.[10] HG-[Leu]Alm may also be dimerized in the presence of Zn^{2+} in membranes, which may cause a significant decrease in leakage. Therefore, we synthesized CG-Alm and CG-[Leu]Alm, each bearing a cysteine at the N-terminus. Disulfide crosslink formation by air oxidation of these peptides yielded a CG-Alm dimer and a CG-[Leu]Alm dimer (Fig. 3A), and their membrane-permeabilizing activities were examined by ANTS/DPX leakage assay (Fig. 3B and C).

The leakage modes of non-crosslinked CG-Alm and CG-[Leu]Alm monomers, measured in buffer containing 1 mM dithiothreitol (DTT), were very similar to those of the corresponding HG-peptides in the absence of Zn^{2+}. CG-Alm monomer induced 50% leakage in the P/L range 0.01–0.02 (Fig. 3B), while CG-[Leu]Alm monomer induced 50% leakage in the P/L range 0.0001–0.0004 (Fig. 3C). Considerable changes in leakage modes were observed by homodimer formation via disulfide-crosslinking in CG-Alm and CG-[Leu]Alm peptides, and these results coincided with those for the corresponding HG-peptides with addition of Zn^{2+}. CG-Alm dimer induced 50% leakage in the P/L range 0.001–0.005, which was about one order of magnitude lower than that for the monomer (Fig. 3B). CG-[Leu]Alm dimer showed extremely low permeabilizing activity (Fig. 3C).

The response of ANTS/DPX leakage from liposomes by HG-Alm to Zn^{2+} corresponded well to that of the channel current levels; i.e., increased levels of ANTS/DPX leakage and ion channel current by HG-Alm were detected in the presence of Zn^{2+} (Fig. 2 and reference number).[10] As the channel formation behavior and induction of ANTS/DPX leakage from liposomes should share a number of similarities, we next analyzed the channel activities of CG-Alm,

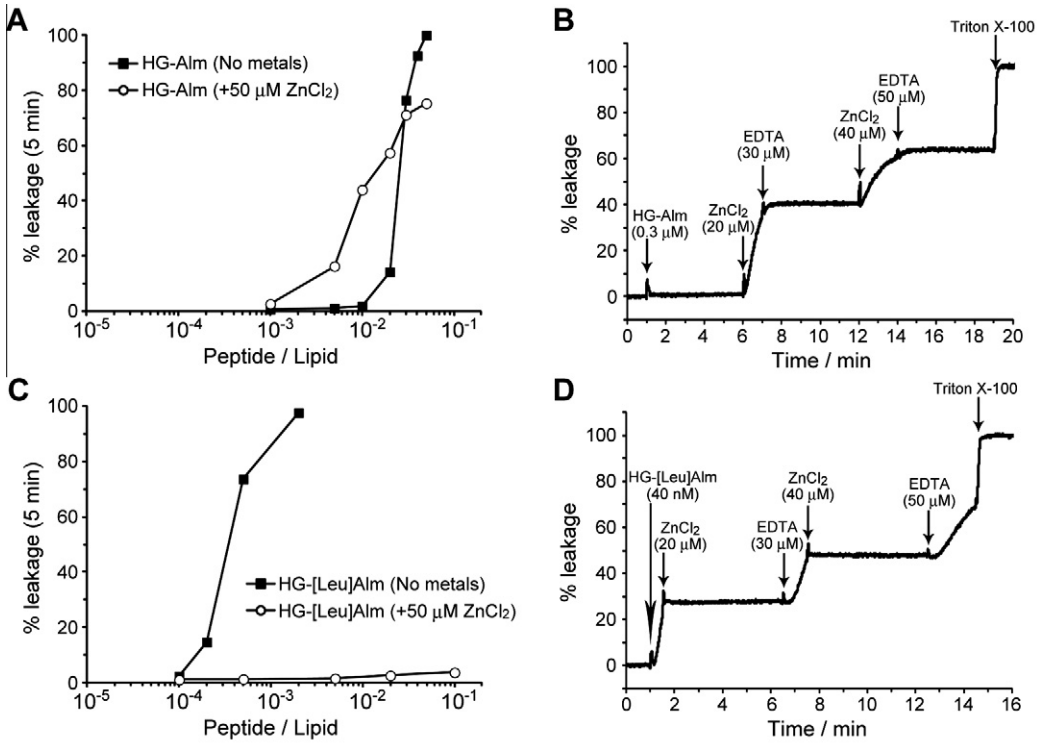

Figure 2. (A, C) The percent leakage of ANTS/DPX from 100% POPC LUVs 5 min after the addition of HG-Alm (A) and HG-[Leu]Alm (C) plotted as a function of peptide / lipid ratio (P/L) in the absence or presence of 50 μM Zn^{2+}. Each data point represents the average of two experiments. (B, D) Leakage control using HG-Alm (B) or HG-[Leu]ALm (D) by the addition and removal of Zn^{2+}. Buffer; 10 mM HEPES, 150 mM NaCl, and 10 μM EDTA (pH 7.4).

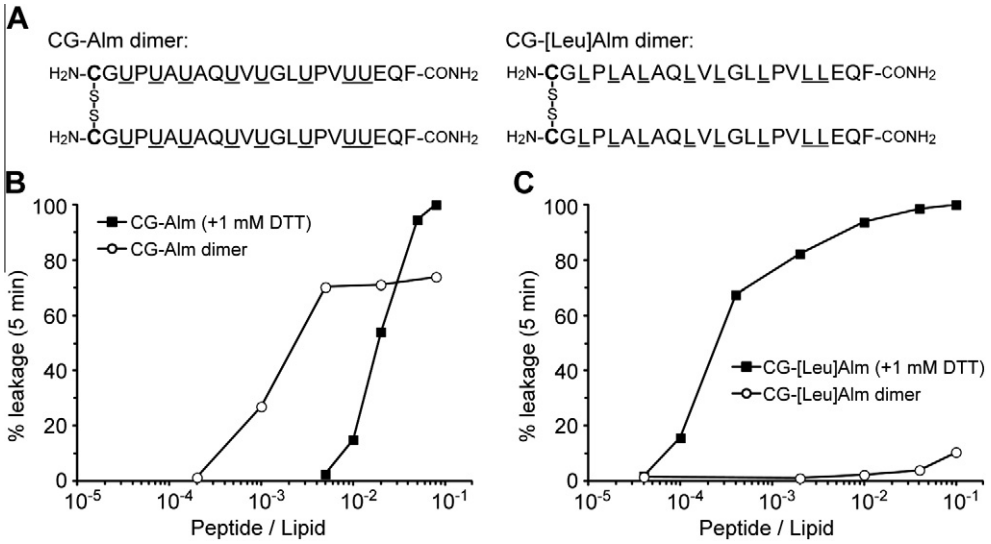

Figure 3. (A) The structures of CG-Alm dimer and CG-[Leu]Alm dimer. (B, C) The percent leakage of ANTS/DPX from 100% POPC LUVs 5 min after the addition of CG-Alm species (B) and CG-[Leu]Alm species (C) plotted as a function of P/L. Each data point represents the average of two experiments. The peptide concentration of the dimeric species are expressed as concentrations of monomers.

CG-[Leu]Alm, and their homodimers by the planar lipid bilayer method (Fig. 4). Fig. 4A and C show the single-channel current measurements of CG-Alm and CG-[Leu]Alm monomers, respectively. Both peptides produced similar channel behaviors with discrete channel conductance levels, except that the channel lifetime of CG-[Leu]Alm was about one order of magnitude shorter than that of CG-Alm, as reported previously for Alm-dUL.[17] The multi-conductance levels were considered to be due to the spontaneous and repetitive uptake and release of helical monomers into and from a channel assembly in the membrane.[18,19]

As observed for HG-Alm and HG-[Leu]Alm, there was a marked difference in the effect of dimerization via disulfide crosslinking for CG-Alm and CG-[Leu]Alm. The CG-Alm dimer produced a channel with major conductance levels of ~3.5 nS and ~6.8 nS with a longer open duration than the monomer (Fig. 4B), as reported previously.[20,21] These major conductance levels were deduced to be for 8-mer and 10-mer assemblies of monomers, respectively, by analogy to the previously reported channel conductance of Alm.[20] Stabilization of higher conductance levels by crosslink formation is compatible with the increment of membrane

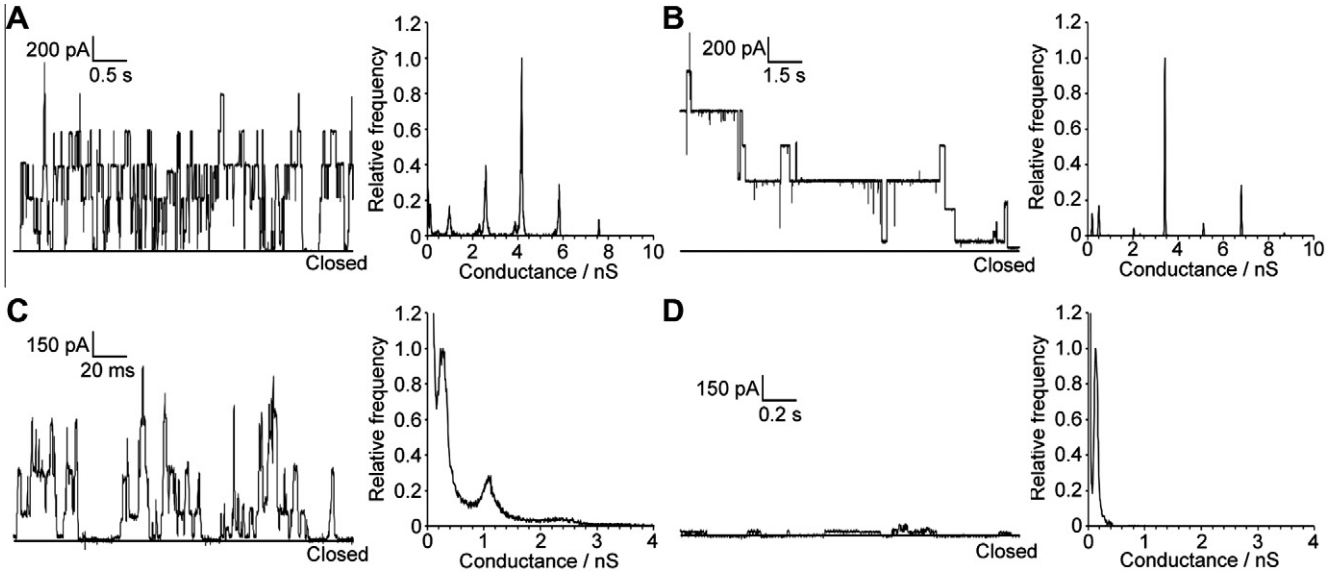

Figure 4. Channel current records and conductance histograms of CG-Alm (A), CG-Alm dimer (B), CG-[Leu]Alm (C), and CG-[Leu]Alm dimer (D). Voltage: 160 mV; electrolyte: 1 M KCl containing 20 mM HEPES, and 0.2 mM EDTA (pH 7.4). When we analyze channel activities of monomer species, 10 mM DTT was added to the electrolyte solution to prevent oxidation.

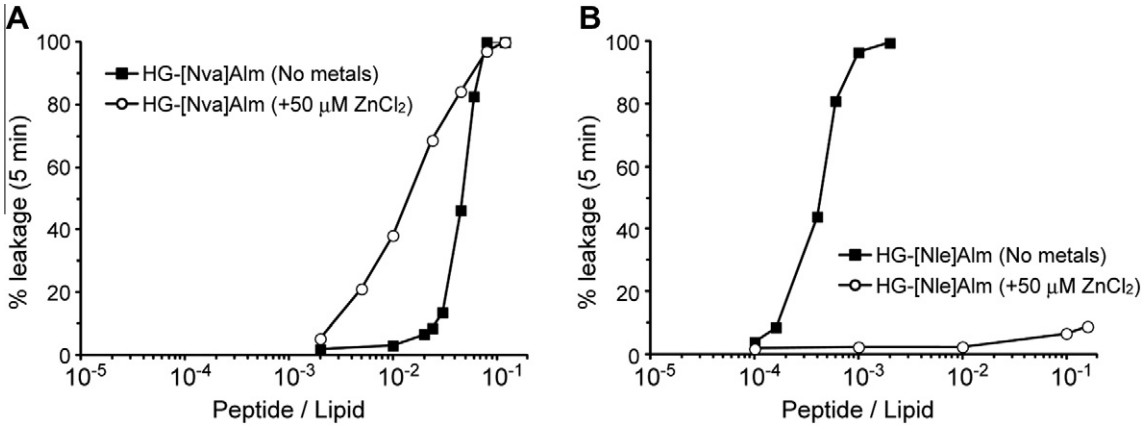

Figure 5. The percent leakage of ANTS/DPX from 100% POPC LUVs 5 min after the addition of HG-[Nva]Alm (A) and HG-[Nle]Alm (B) plotted as a function of P/L in the absence or presence of 50 μM Zn^{2+}. Each data point represents the average of two experiments. Buffer; 10 mM HEPES, 150 mM NaCl, and 10 μM EDTA (pH 7.4).

permeability of HG-Alm seen in the presence of Zn^{2+}. On the other hand, crosslink formation in CG-[Leu]Alm predominantly produced channels with lower conductance (~0.13 nS) (Fig. 4D), which coincided with the conductance of the template assembled Alm tetramer.[22] Although some increase in channel open duration for the conductance level of ~0.13 nS was observed, the channel open duration was significantly shorter than that for the CG-Alm dimer.

2.4. Other Aib-substituted HG-Alm analogs

By Fourier transform infrared (FTIR) spectroscopy, Haris et al. showed that replacement of all Aib residues in Alm with leucine increased the interaction with the membrane, and stabilized its helical structure.[23] This difference in membrane affinity may be responsible for the difference in the leakage behavior of HG-Alm from HG-[Leu]Alm as a response to addition of metal ions. Therefore, we selected Nva and Nle as substituents of Aib to examine the effects of substitution with different amino acids with preferable effects on helical formation but with different hydrophobicities; Nva and Nle are both strong helix-promoting amino acids.[24] Nva and Nle have no branched aliphatic side chains and have three and four carbons, respectively. HG-[Nva]Alm and HG-[Nle]Alm (Fig. 1) were prepared using standard Fmoc-solid-phase peptide synthesis without difficulty, and the effects of Zn^{2+} on leakage-promoting activity were examined (Fig. 5).

Fig. 5A shows the results for HG-[Nva]Alm. In the absence of Zn^{2+}, 50% leakage was observed in the P/L of ~0.045, while in the presence of 50 μM $ZnCl_2$ the same extent of leakage was induced in the P/L range of 0.01–0.024, showing a similar tendency to that of HG-Alm. In contrast, addition of 50 μM $ZnCl_2$ resulted in a considerable decrease in the membrane-permeabilizing activity of HG-[Nle]Alm (Fig. 5B), as seen in the case of HG-[Leu]Alm. In the absence of Zn^{2+}, 50% leakage was induced in the P/L range 0.0004–0.0006, while only ~7% leakage was induced even at the P/L of 0.1 in the presence of 50 μM $ZnCl_2$. Similar methods of Zn^{2+}-mediated sequential switch of ANTS/DPX leakage were performable using HG-[Nva]Alm and HG-[Nle]Alm instead of HG-Alm and HG-[Leu]Alm, respectively (Supplementary data Fig. 2).

We also synthesized an analog of HG-Alm in which all the Aib residues were substituted with α-aminobutyric acid (Abu),

HG-[Abu]Alm (Supplementary data Fig. 3A). Abu has an ethyl group as the side chain, which has a lower hydrophobicity than Nva. Leakage experiments indicated that HG-[Abu]Alm had a much lower membrane-permeabilizing activity than HG-Alm or HG-[Nva]Alm; less than 5% leakage was induced at even the P/L of 0.5, regardless of Zn^{2+} (Supplementary Fig. 3B).

2.5. Changes in the CD spectra induced by Zn^{2+}

Finally, we examined Zn^{2+}-mediated changes in the secondary structure of HG-Alm and its analogs by measuring the CD spectra in the presence of POPC LUVs (Fig. 6). In the absence of Zn^{2+}, all of the peptides yielded a spectrum with local minima at ~208 and ~222 nm, indicative of a helical structure. Addition of 200 μM Zn^{2+} caused a significant increase in the $[\theta]_{222}$ of HG-Alm and HG-[Nva]Alm ($[\theta]_{222}$: -0.92×10^4 to -1.22×10^4 deg cm^2 dmol^{-1}, -0.47×10^4 to -1.37×10^4 deg cm^2 dmol^{-1}, respectively) (Fig. 6A and C). On the other hand, addition of 200 μM Zn^{2+} caused no apparent changes in the CD spectra of HG-[Leu]Alm and HG-[Nle]Alm ($[\theta]_{222}$: -1.23×10^4 to -1.20×10^4, -1.09×10^4 to -1.14×10^4 deg cm^2 dmol^{-1}, respectively) (Fig. 6B and D). In addition, HG-[Abu]Alm yielded no significant helical structure in the presence of POPC LUVs regardless of Zn^{2+} (data not shown), suggesting its lack of ability to form stable pores in the membranes.

3. Discussion

In this study, we examined the membrane-permeabilizing activities of Alm analogs bearing an N-terminal His residue; that is, HG-Alm, HG-[Leu]Alm, HG-[Nva]Alm, and HG-[Nle]Alm. These peptides were divided into two classes based on their response to Zn^{2+} in a leakage assay using LUVs containing ANTS and DPX. In the cases of HG-Alm and HG-[Nva]Alm, with shorter side chain lengths than the others, the leakage of ANTS/DPX through the liposomal membranes was greatly accelerated by the addition of Zn^{2+}. On the other hand, while HG-[Leu]Alm and HG-[Nle]Alm allowed leakage of ANTS/DPX from liposomes, Zn^{2+} effectively blocked this leakage. These responses of the respective peptides to Zn^{2+} were reversible; repeated addition and removal of Zn^{2+} with EDTA led to successive switching on and off of ANTS/DPX leakage through the liposomal membranes.

A salient difference in the response in the CD spectra to the addition of Zn^{2+} was found between these two classes of peptide in the presence of liposomes. Significant enhancement of helical structures was observed for HG-Alm and HG-[Nva]Alm with the addition of Zn^{2+}. However, Zn^{2+} yielded no significant differences in the CD spectra of HG-[Nle]Alm and HG-[Leu]Alm, and these differences were consistent with their responses with regard to ANTS/DPX leakage.

Our previous study using single-channel recording of HG-Alm suggested the formation of its dimer structures in the presence of Zn^{2+}, stabilizing the assembly of HG-Alm in the membranes and leading to an increase in channel current.[10] Stabilization of the Alm assembly in the membranes was also reported for alamethicin pyromellitate in the presence of calcium.[5] The stabilization of the HG-Alm assembly by Zn^{2+} facilitated the assembly of larger numbers of HG-Alm spanning membranes, which led to an increase in the helical tendency of the peptide, as determined by CD, and a greater flux of ANTS/DPX through the liposomal membranes.

The possible promotion of ANTS/DPX leakage by the Zn^{2+}-mediated stabilization of HG-Alm assembly was further supported by studies of membrane-permeabilizing activities and ion channel activities of the disulfide crosslinked dimer of CG-Alm in comparison with its non-crosslinked monomer. Crosslink formation considerably enhanced ANTS/DPX leakage through the liposomal membranes. The CG-Alm dimer produced a longer-lived channel current due to stabilization of the assembly states, which may correspond to the 8- and 10-mer assemblies of CG-Alm.

Further detailed studies are required to determine why addition of Zn^{2+} to HG-[Leu]Alm and HG-[Nle]Alm led to inhibition of ANTS/DPX leakage. It should be noted that, although there was no significant alteration in the helical content of these peptides upon the addition of Zn^{2+}, the helical contents of HG-[Leu]Alm and HG-[Nle]Alm based on the molar ellipticity $[\theta]_{222}$ were similar to

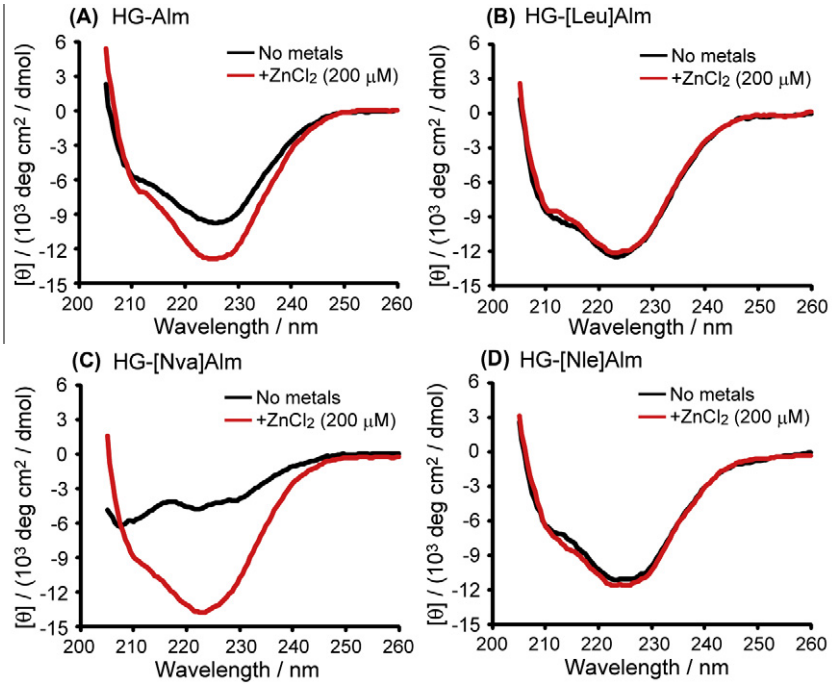

Figure 6. CD spectra of the HG-Alm analogs. Buffer; 10 mM HEPES, 150 mM NaCl, and 0.1 mM EDTA (pH 7.4). Liposomes; 100% POPC LUV ([Lipid] = 1 mM). Peptide concentration; 25 μM. Buffer; 10 mM HEPES, 150 mM NaCl, and 10 μM EDTA (pH 7.4).

those obtained for HG-Alm and HG-[Nva]Alm in the presence of Zn^{2+}. In addition, the P/L required for 50% leakage for HG-[Leu]Alm and HG-[Nle]Alm-treated liposomes was almost two orders of magnitude lower than those for HG-Alm and HG-[Nva]Alm-treated liposomes (Figs. 2 and 5, respectively), suggesting the greater incorporation of HG-[Leu]Alm and HG-[Nle]Alm into the membranes. These results suggest that HG-[Leu]Alm and HG-[Nle]Alm, which are more hydrophobic than the other peptides, may more easily form transmembrane assembly structures, which may allow ANTS/DPX leakage even in the absence of Zn^{2+}. It has been reported that even a hydrophobic helical peptide without the expected specific side chain interactions, acetyl-$(LALAAAA)_3$-NH_2, forms aggregates in the membrane.[25] Thus the longer side chains of the former peptides may have been more favorable for the formation of stable and compact helix assemblies.

Assuming that HG-[Leu]Alm and HG-[Nle]Alm may already have a stable helical structure in the membrane in the absence of Zn^{2+}, the addition of Zn^{2+} should yield a tighter assembly of helical peptides via pseudo-crosslink formation caused by complex formation of Zn^{2+} with His residues, resulting in a decrease in ANTS/DPX permeation through the membranes. Single-channel measurement of CG-[Leu]Alm showed that channel formation by this peptide was of a much shorter duration and lower levels of open-channel conductance than the non-crosslinked CG-Alm monomer. Disulfide crosslink formation in CG-[Leu]Alm yielded a decrease in the channel conductance level of ~0.13 nS, presumably due to tetramer assembly of [Leu]Alm molecules. Since Leu has a longer and more hydrophobic aliphatic side chain than Aib, the helix diameter of [Leu]Alm may not be identical to that of Alm. However, the observed conductance levels for monomeric CG-[Leu]Alm were shared with those of monomeric CG-Alm (e.g., 0.25, 1.1, 2.4 nS), and there may not be marked differences in the conductance of the channels formed by these peptides. The radius of the pore formed by tetrameric bundles of [Leu]Alm was estimated to be ~0.2 nm by analogy to Alm channels using the equation presented by Sansom[19], which is an insufficient size for ANTS/DPX leakage.[15,26]

4. Conclusions

In this study, HG-Alm analogs, in which all Aib residues were substituted with Leu, Nva, or Nle, were synthesized and their membrane-permeabilizing activities were examined by ANTS/DPX leakage assay. The responses to Zn^{2+} differed according to the differences in the side chains of the substitute amino acids, and demonstrated the feasibility of controlling the membrane-permeabilizing activities of these peptides by addition or removal of Zn^{2+}.

Further studies are required to clarify why such substitution of Aib in the HG-Alm sequence yields completely different behaviors with regard to the presence or absence of Zn^{2+}. However, the observations in the present study have implications for the methodological understanding of the assembly formation of membrane proteins as well as for the design of artificial membrane proteins with gating functions.

5. Experimental section

5.1. Peptide synthesis

All the peptides employed in this study were prepared using Fmoc (=9-fluorenylmethyloxycarbonyl)-solid-phase peptide synthesis. Peptide-chain construction of Aib-containing Alm analogs was conducted using the fluoride activation method of Fmoc-amino acid derivatives as previously reported.[10] Other peptides without containing Aib were prepared using ordinary Fmoc-solid-phase methods. Details about the preparation of these peptides are described in Supplementary data.

5.2. Vesicle preparation

For preparation of liposomes containing ANTS and DPX, a thin film of POPC (NOF corporation, Tokyo, Japan) after drying under vacuum overnight was hydrated with buffer A (12.5 mM ANTS, 40 mM DPX, 10 mM HEPES, and 70 mM NaCl, pH 7.4) and vortex-mixed to produce multilamellar vesicles (MLVs). The suspension was freeze-thawed for five cycles, followed by multiple extrusions (31 times) through a 100 nm pore size polycarbonate membrane using a LiposoFast device (Avestin, Ottawa, Canada) to produce LUVs. Extravesicular dyes were removed by gel filtration (Sephadex G-25, GE healthcare) with buffer B (10 mM HEPES and 150 mM NaCl, pH 7.4). For preparation of liposomes for CD measurements, buffer B was used instead of buffer A. Lipid concentrations were estimated by choline oxidase-DAOS method, using Phospholipids C kit (Wako Pure Chemicals, Osaka, Japan).

5.3. Channel activity measurements

Planar lipid bilayers were formed from diphytanoylphosphatidylcholine (Avanti, Alabaster, AL, USA) by the monolayer-folding method.[27] A small quantity (usually 1–10 μL) of peptides in CH_3OH was added to the electrolyte solutions (1 mL) on one side of the membrane (designated as the cis side) to obtain each final concentration. A pair of Ag-AgCl electrodes was used for current measurement and voltage supply. The *cis*- and *trans*-side electrodes were connected to a DC voltage source and to the virtual ground of an in-house-made current amplifier, respectively. The output voltages of the current amplifier were recorded with a DL708 8 CH Digital Scope (Yokogawa, Tokyo, Japan) with sampling frequency of 20 kHz after filtering at 4 kHz (Fig. 4C) or 2 kHz after filtering at 0.4 kHz (Fig. 4A, B and D). All channel current records in this study were carried out at 24 ± 1 °C. Conductance histograms were calculated from channel current records for 5 s (Fig. 4A), 10 s (Fig. 4C), or 20 s (Fig. 4B and D).

5.4. Fluorescence measurements

ANTS fluorescence emission spectra were recorded at 515 nm with excitation at 353 nm on a spectrofluorophotometer, RF-5300 (Shimadzu, Kyoto, Japan) with a cuvette holder thermostated at 25 °C. The excitation and emission bandwidths were 5 nm. A quartz cuvette of 1 cm light-path length, equipped with a magnetic stirrer, was filled with 2 mL buffer solution (10 mM HEPES, 150 mM NaCl, and 10 μM EDTA, pH 7.4) with liposomes. The lipid concentration was kept constant at 50 μM and 20 μL of peptides in CH_3OH or CF_3CH_2OH was added to the solution to obtain each final peptide-to-lipid molar ratio (P/L). For the leakage control experiments (Fig. 2B, D and Supplementary data Fig. 2), 10 μL of $ZnCl_2$ or EDTA solution (2–10 mM) was added to the solution. The maximum fluorescence intensity corresponding to 100% leakage was determined by the addition of 10% w/v Triton X-100 (20 μL) to the sample. The apparent percent leakage value t min after the addition of peptides, $L(t)$, was calculated according to Eq. 1,

$$L(t) = 100(F(t) - F_o)/(F_{tot} - F_o) \quad (1)$$

where F_{tot} denotes the fluorescence intensity after addition of Triton X-100. F_o and $F(t)$ represent the fluorescence before and t min after addition of peptides, respectively.

5.5. Circular dichroism (CD) measurements

The CD spectra were recorded on a Jasco J-820 spectropolarimeter at 25 °C in a 0.1 cm path length cell under a nitrogen atmosphere. Each CD spectrum represents an average of 8 scans, obtained at 0.5 nm intervals between 200 and 260 nm with a scanning speed of 100 nm min^{-1}.

Acknowledgments

This work was supported by Grants-in-Aid for Scientific Research from the Ministry of Education, Culture, Sports, Science and Technology of Japan. D. N. received a JSPS Research Fellowship for Young Scientists.

Supplementary data

Supplementary data associated with this article can be found, in the online version, at http://dx.doi.org/10.1016/j.bmc.2012.09.046.

References and notes

1. Leitgeb, B.; Szekeres, A.; Manczinger, L.; Vágvölgyi, C.; Kredics, L. *Chem. Biodivers.* **2007**, *4*, 1027.
2. Fox, R. O., Jr.; Richards, F. M. *Nature* **1982**, *300*, 325.
3. Hall, J. E.; Vodyanoy, I.; Balasubramanian, T. M.; Marshall, G. R. *Biophys. J.* **1984**, *45*, 233.
4. Cafiso, D. S. *Annu. Rev. Biopys. Biomol. Struct.* **1994**, *23*, 141.
5. Woolley, G. A.; Epand, R. M.; Kerr, I. D.; Sansom, M. S. P.; Wallace, B. A. *Biochemistry* **1994**, *33*, 6850.
6. Schmitt, J. D.; Sansom, M. S. P.; Kerr, I. D.; Lunt, G. G.; Eisenthal, R. *Biochemistry* **1997**, *36*, 1115.
7. Zhang, Y.; Futaki, S.; Kiwada, T.; Sugiura, Y. *Bioorg. Med. Chem.* **2002**, *10*, 2635.
8. Kiwada, T.; Sonomura, K.; Sugiura, Y.; Asami, K.; Futaki, S. *J. Am. Chem. Soc.* **2006**, *128*, 6010.
9. Mayer, M.; Semetey, V.; Gitlin, I.; Yang, J.; Whitesides, G. M. *J. Am. Chem. Soc.* **2008**, *130*, 1453.
10. Noshiro, D.; Asami, K.; Futaki, S. *Biophys. J.* **2010**, *1801*, 98.
11. Ritov, V. B.; Murzakhmetova, M. K.; Tverdislova, I. L.; Menshikova, E. V.; Butylin, A. A.; Avakian, T. Y.; Yakovenko, L. V. *Biochim. Biophys. Acta* **1993**, *1148*, 257.
12. Fisher, M. B.; Campanale, K.; Ackermann, B. L.; Vandenbranden, M.; Wrighton, S. A. *Drug Metab. Dispos.* **2000**, *28*, 560.
13. Kropacheva, T. N.; Raap, J. *Chem. Biodivers.* **2007**, *4*, 1388.
14. Scrimin, P.; Tecilla, P.; Tonellato, U.; Veronese, A.; Crisma, M.; Formaggio, F.; Toniolo, C. *Chem. Eur. J.* **2002**, *8*, 2753.
15. Parente, R. A.; Nir, S.; Szoka, F. C., Jr. *Biochemistry* **1990**, *29*, 8720.
16. Karle, I. L.; Balaram, P. *Biochemistry* **1990**, *29*, 6747.
17. Moue, G.; Duclohier, H.; Dugast, J. Y.; Spach, G. *Biopolymers* **1989**, *28*, 273.
18. Woolley, G. A. *Chem. Biodivers.* **2007**, *4*, 1323.
19. Sansom, M. S. P. *Prog. Biophys. Mol. Biol.* **1991**, *55*, 139.
20. Okazaki, T.; Sakoh, M.; Nagaoka, Y.; Asami, K. *Biophys. J.* **2003**, *85*, 267.
21. You, S.; Peng, S.; Lien, L.; Breed, J.; Sansom, M. S. P.; Woolley, G. A. *Biochemistry* **1996**, *35*, 6225.
22. Futaki, S.; Fukuda, M.; Omote, M.; Yamauchi, K.; Yagami, T.; Niwa, M.; Sugiura, Y. *J. Am. Chem. Soc.* **2001**, *123*, 12127.
23. Haris, P. I.; Molle, G.; Duclohier, H. *Biophys. J.* **2004**, *86*, 248.
24. Lyu, P. C.; Sherman, J. C.; Chen, A.; Kallenbach, N. R. *Proc. Natl. Acad. Sci. U.S.A.* **1991**, *88*, 5317.
25. Yano, Y.; Takemoto, T.; Kobayashi, S.; Yasui, H.; Sakurai, H.; Ohashi, W.; Niwa, M.; Futaki, S.; Sugiura, Y.; Matsuzaki, K. *Biochemistry* **2002**, *5*, 3073.
26. Hanke, W.; Boheim, G. *Biochim. Biophys. Acta* **1980**, *596*, 456.
27. Asami, K.; Okazaki, T.; Nagai, Y.; Nagaoka, Y. *Biophys. J.* **2002**, *83*, 219.